

ANALYSIS OF CURRENT- INDUCED FORCES ON OFFSHORE PIPELINE BUNDLES

M H KAMARUDIN¹, K P THIAGARAJAN^{2†}, A CZAJKO³

^{1,2} School of Oil & Gas Engineering, University of Western Australia, Crawley, WA 6009

³J P Kenny Pty Ltd., Perth, Western Australia 6000

ABSTRACT

Offshore pipelines are often accompanied by smaller diameter service lines or umbilicals to create a bundle. The flow behaviour around a pipeline bundle is complex and not well known and this leads to the concern on the stability of the configuration. This paper investigates the influence of the piggyback pipeline on the hydrodynamic loading of the bundle in steady current flow using a Computational Fluid Dynamics (CFD) package, FLUENT. The research undertaken is compared against established industry practice of assuming that the hydrodynamic characteristics for the bundle are the same as an equivalent diameter cylinder. Key parameters of the configuration that were investigated were the orientation of the smaller pipe with respect to the main pipeline, and the flow conditions. The gap between the seabed and the main pipe was set to zero for all cases investigated. The results of the numerical analyses showed that the presence of the piggyback has a significant influence on the hydrodynamic characteristics of the main pipe. The Equivalent Diameter approach adopted in engineering design may underestimate the forces on the bundle. It was also found that the orientation of the piggyback plays an essential role in determining the drag and lift coefficients for the bundle. This phenomenon is better understood by examining the pressure distribution around the cylinder.

NOMENCLATURE

A	frontal area of cylinder
β	reference location of the small cylinder with respect to the main cylinder
C_D	drag coefficient
C_L	lift coefficient
C_p	pressure coefficient
d	diameter of the small cylinder
D	diameter of the main cylinder
e	gap between main cylinder and seabed
\overline{F}_D	drag force
\overline{F}_L	lift force
G	gap between main cylinder and small cylinder
p	pressure
Re	Reynolds number

U	horizontal current induced velocity
ρ	density of fluid (water)

INTRODUCTION

Offshore pipelines are usually subject to wave and current loading. This will exert forces on the pipelines which later may result in pipeline failure if the design limits are exceeded. Many offshore pipelines are accompanied by a smaller diameter service line or umbilical to create a bundle. It is expected that the existence of the piggyback pipeline may have some effects on the hydrodynamic forces of the main pipeline. The flow behaviour around a pipeline bundle is complex and not well known and this leads to concern on the stability of the configuration. This in turn may require some modifications in pipeline configuration to ensure that the piggyback pipeline is stable. This may be achieved by increasing the mass of the pipelines via a concrete weight coating or increased wall thickness (DNV, 1988). However, this can result in significant cost and may adversely affect pipeline handling and installation. Thus, a fundamental need was identified for detailed examination of the external hydrodynamic loading on this type of configuration. We consider in this paper the influence of current only loading. Instabilities in loading such as due to combined waves and currents will be discussed in a forthcoming paper by the authors.

Pipelines exposed to a steady current will experience an in-line force as well as a transverse force. The magnitude of these forces depends on the Reynolds number. This is due to the importance of the boundary layer in the viscous region around the pipe surface. The contribution of the in-line and the transverse forces are the results of the skin friction and also the pressure distribution around the pipe that act in-line and normal to the flow respectively. They can be represented as;

$$\begin{aligned}\overline{F}_D &= \frac{1}{2} \rho C_D A U |U| \\ \overline{F}_L &= \frac{1}{2} \rho C_L A U |U|\end{aligned}\quad (1)$$

where symbols are defined in the nomenclature. Even though much theoretical and experimental research has

[†] Corresponding author

¹ Now with INTEC Engineering, Perth

been done to study the hydrodynamic characteristics on twin and multiple cylinder configurations, most appears to be confined to cylinders of equal diameter. Very little information is available on the effect of hydrodynamic forces on the main pipeline with a piggyback configuration. Due to this lack of knowledge, the optimum design parameters that minimise the total forces are not well-known. The design practice of a piggyback configuration adopts an equivalent diameter approach whose validity has not been extensively researched. This approach assumes that the hydrodynamic load on a piggyback configuration is equivalent to a single cylinder whose diameter is the sum of the diameters of the main and piggyback plus the gap in between. In this paper, we use a computational approach to model a piggyback cylinder and compare the loads on an equivalent diameter cylinder. The influence of different parameters of the configuration on this comparison is studied.

MODEL DESCRIPTION

Computational Domain

A 2D numerical domain (Figure 1) was created to represent the model and its vicinity. Consideration was given to the grid around the wall of the cylinder and its ability to capture the interactions between the vortices that may contribute to the hydrodynamic forces. The inlet boundary was set far enough in front of the cylinder to allow the flow to be fully developed by the time the flow reaches the cylinder. The minimum inlet distance was set at ten times the diameter of the main cylinder (10D). An outflow boundary condition with no back pressure limitation was found to be suitable when the exit flow is in a fully developed condition. A downstream distance of twenty times the diameter of the main cylinder (20D) was chosen. Ten times the diameter of the main cylinder (10D) was specified to be the height of the computational domain.

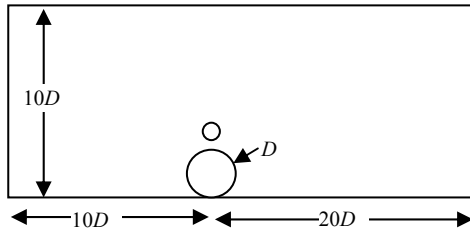


Figure 1: Geometry of Computational Domain

Modelling Turbulence

After some validation process, the Standard k-ε model with Enhanced Wall Treatment was chosen for this research. This is a semi-empirical model based on model transport equations for the turbulence kinetic energy (k) and its dissipation rate (ε). In the derivation of the k-ε model, it is assumed that the flow is fully turbulent, and the effects of molecular viscosity are negligible (FLUENT, 2003). The following transport equation for turbulence kinetic energy, k, and the rate of dissipation, ε provide the necessary closure of the Navier-Stokes equations:

$$\frac{\partial}{\partial t}(\rho k) + \frac{\partial}{\partial x_i}(\rho k u_i) = \frac{\partial}{\partial x_j} \left[\left(\mu + \frac{\mu_t}{\sigma_k} \right) \frac{\partial k}{\partial x_j} \right] + G_k + G_b - \rho \varepsilon - Y_M + S_k \quad (2)$$

and

$$\frac{\partial}{\partial t}(\rho \varepsilon) + \frac{\partial}{\partial x_i}(\rho \varepsilon u_i) = \frac{\partial}{\partial x_j} \left[\left(\mu + \frac{\mu_t}{\sigma_\varepsilon} \right) \frac{\partial \varepsilon}{\partial x_j} \right] + C_{1\varepsilon} \frac{\varepsilon}{k} (G_k + C_{3\varepsilon} G_b) - C_{2\varepsilon} \rho \frac{\varepsilon^2}{k} + S_\varepsilon \quad (3)$$

Where G_k and G_b = turbulence kinetic energy due to the mean velocity gradients and buoyancy respectively

Y_M = contribution of the fluctuating dilatation in compressible turbulence to the overall dissipation rate

σ_k and σ_ε = turbulent Prandtl numbers

S_k and S_ε = optional user-defined source terms (not used here)

$C_{2\varepsilon}$ and $C_{3\varepsilon}$ = constants

Further details may be had from FLUENT (2003).

The numerical model was validated for uniform flow past a singular cylinder. The cylinder diameter was 0.508m, and the Reynolds number ranged from 10 to 3.6×10^6 . The computational domain was discretised into 113910 structured mesh elements. The cylinder was located at the mid-height of the computational domain. Symmetric boundary conditions were prescribed on the two lateral boundaries. The drag coefficients computed were compared with Schlichting (1979) and found to agree within 10%. However, it has been found that the model fails to capture the drag crisis region between $3.5 \times 10^5 < Re < 1.5 \times 10^6$ where the transition from laminar to turbulent boundary layer occurs. As a further validation, flow past a cylinder resting on the seabed was simulated for Reynolds number of 1×10^4 . The drag coefficient was found to be lower than the free stream case, in agreement with experimental results by Jensen, et. al.(1990) and Kiya, M. (1968) (as cited in Sumer and Fredsoe, 1997). Further validation details may be found in Kamarudin (2005).

Description of Model Configurations

In this study, the influence of piggyback on the main cylinder is investigated. The main cylinder is fixed to the sea bottom ($e/D=0$) while the piggyback is situated at different orientations, Figure 2. The gap ratio between the main cylinder and the piggyback (G/D) is kept constant

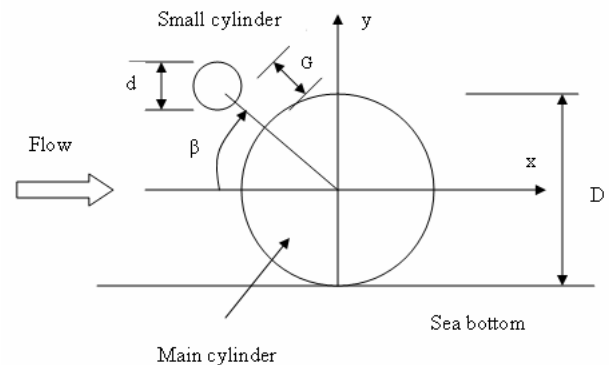
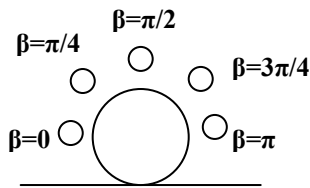


Figure 2: Model Definition

at 0.1. The diameter ratio of the small cylinder (d) to the main cylinder (D) is set to constant value of 0.2. The diameter of the main pipe and the smaller pipe were chosen as 0.508m (20") and 0.1016m (4") respectively.

Five orientations of piggyback configurations were simulated with $\beta=0, \pi/4, \pi/2, 3\pi/4$ and π as defined in Figure 2. These configurations were based on commonly used designs in the industry. The Reynolds numbers simulated were 300, 1000, 10000, 1.4×10^5 and 7.5×10^5 .



RESULTS

Force Coefficients on Main Cylinder

Figures 3 and 4 show the variations of the force coefficients on the main cylinder at different Reynolds numbers and piggyback configurations. For the purpose of comparison, the force coefficients on the single cylinder without the piggyback are also plotted. It can be seen that the main cylinder experiences maximum mean drag coefficient when the small cylinder is on top of the main cylinder ($\beta=\pi/2$) for all Reynolds numbers investigated. The mean drag coefficient for this configuration is higher by around 30%-50% than the single cylinder. The drag increase for the $\beta=\pi/2$ arrangement is mainly caused by the increase of the stagnation pressure and the high pressure region in downstream of the cylinder. This can be better explained by observing the mean pressure distributions along the perimeter of the cylinder which will be carried out in the later section. With other piggyback configurations, the change in the mean drag coefficients on the main cylinder is not that dramatic as compared to its single cylinder counterpart. However, it is interesting to note that for $\beta=0$ and $\beta=\pi$, the mean drag coefficients on the main cylinder are actually smaller than the single

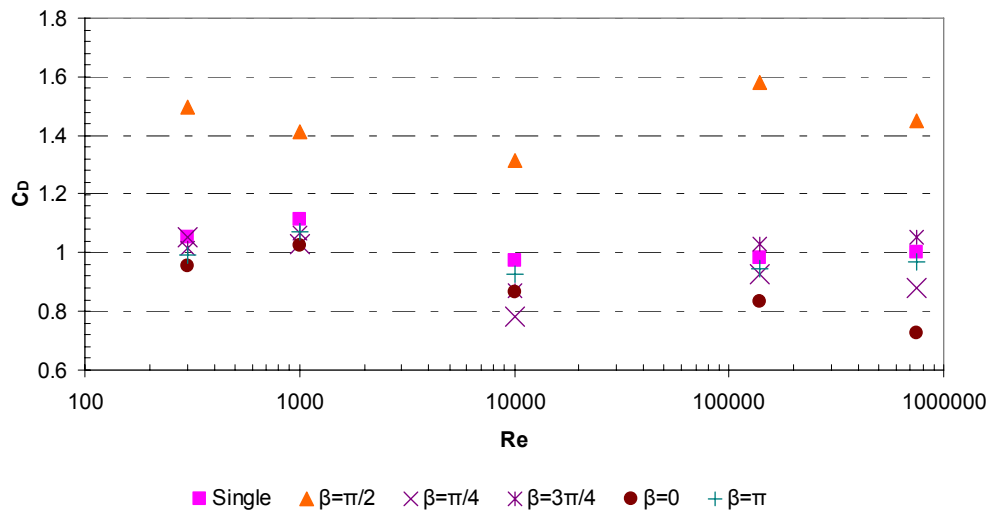


Figure 3: Mean Drag Coefficients for Main Cylinder

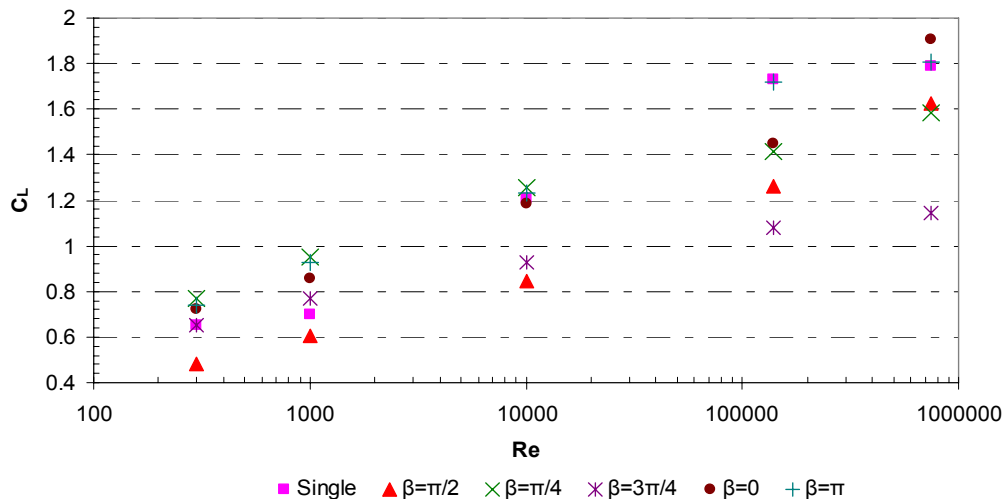


Figure 4: Mean Lift Coefficients for Main Cylinder

cylinder. The arrangement of $\beta=0$ experiences 28% reduction in drag compared to the $\beta=\pi$ arrangement at higher Reynolds numbers. This reduction is mainly due to a combination of the decrease in stagnation pressure and increase in the base pressure of the main cylinder when the small cylinder is placed in front of the stagnation point of the main cylinder (Zhao et. al., 2005). For $\beta=\pi$ arrangement, the small cylinder is placed in the wake region of the main cylinder. The formation of the upper shear layer of the main cylinder and the interactions of the shear layers of the main cylinder will increase the base pressure. This happens as a result of the interference of the small cylinder (Sakamoto and Haniu, 1994). This phenomenon is better understood because the placement of the small cylinder in side-by-side arrangement is equivalent to attaching a fairing device to the main cylinder that created a streamline shape for the cylinders thus reducing the drag. The reduction in drag is also observed for $\beta=\pi/4$ arrangement at higher subcritical and critical range of Reynolds numbers.

The effects of the small cylinder on the mean lift coefficients for the main cylinder are also as significant as the mean drag. All the lift coefficients obtained are positive (away from the seabed) due to the non-symmetrical nature of the flow as the pipe is resting on the seabed

($e/D=0$). Complementing the increase in the mean drag coefficients, the main cylinder will experience a reduction in the mean lift coefficients by up to 28% with $\beta=\pi/2$ arrangement. This can be explained by recognizing that drag and lift are 90 degrees out of phase. The graph has a consistent trend of increasing lift with increasing Reynolds number. This may be due to the change in the location of the separation point that moves downstream as the flow velocity increases. Figure 4 shows that the maximum lift will occur at $\beta=\pi/4$ arrangement even though there are some inconsistencies at higher Reynolds numbers ($Re=1.4 \times 10^5$ and 7.5×10^5). In majority of the Reynolds number range, the change in lift is negligible as compared to its single cylinder counterpart when the small cylinder is placed in the wake region ($\beta=\pi$).

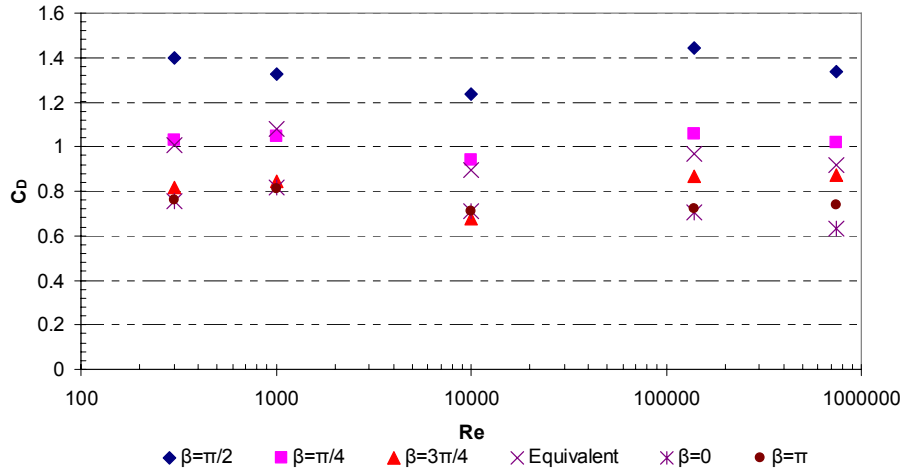
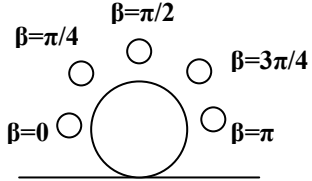


Figure 5: Mean Drag Coefficients for Cylinder Bundle

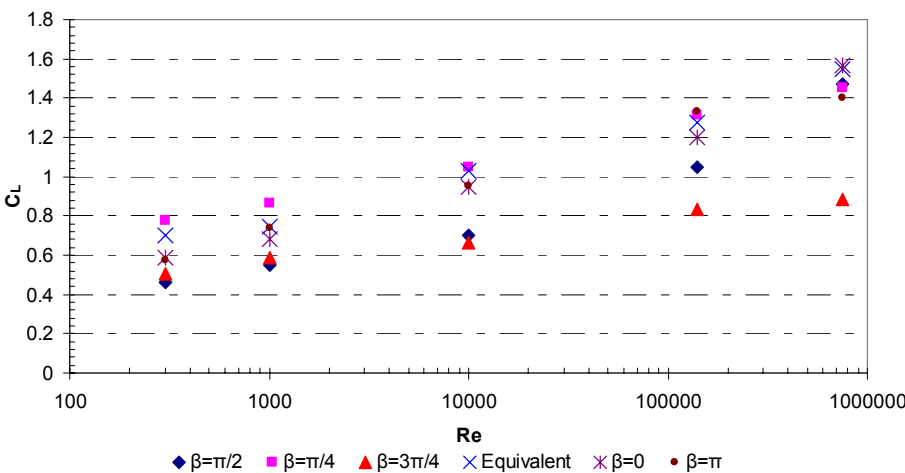


Figure 6: Mean Lift Coefficients for Cylinder Bundle

Force Coefficients on Cylinder Bundle

The total forces of the cylinders are of great importance in pipeline design. It is common practice to simplify the two cylinders as a single cylinder with equivalent diameter ($D_e = D + d + G$). The expectation is that the force coefficients on the equivalent cylinder may be considered as a good conservative representation of the coefficients on the actual configuration. Figures 5 and 6 show the mean drag and the mean lift coefficients for the bundle normalized by the equivalent diameter. For the purpose of comparison, the drag of the equivalent diameter cylinder is also plotted. It can be seen that for $\beta=\pi/2$, the drag on the bundle is about 18%-40% higher than its equivalent counterpart cylinder. This shows that for this configuration one may underestimate the total force on the bundle with the equivalent diameter cylinder approach. However, the assumption corresponds fairly well with $\beta=\pi/4$ arrangement with only 10% of discrepancy. With the remaining configurations, the total drag force on the bundle is lower than that of the equivalent cylinder. It should be noted that the variations of the mean total drag coefficients with piggyback configurations are similar to that of the mean drag on the main cylinder alone (see for details, Kamarudin, 2005). This is due to the fact that the force exerted on the small cylinder is relatively small compared to the main cylinder and thus can be regarded as negligible when computing the coefficients of the bundle.

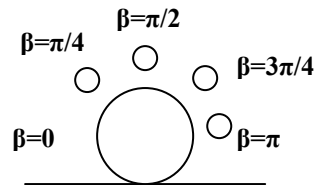
Figure 6 shows the mean total lift coefficients for the cylinders. It is observed that the arrangement of $\beta=3\pi/4$ recorded the minimum lift for the bundle in most of the cases. With regard to validating the equivalent diameter concept, the assumptions match quite well when the small cylinder is placed with $\beta=\pi/4$ only with some small differences in terms of the mean lift. It can also be seen that with this normalization, the small cylinder of $\beta=\pi$ and $\beta=0$ bundle recorded an almost similar drag throughout the Reynolds numbers examined. Similar to the mean total drag coefficients, the mean total lift has the same variations as the main cylinder with different piggyback orientations.

Pressure Distribution along Main Cylinder Surface

Since the variation of the force coefficients are related to the pressure gradient it is important to see the change of the pressure along the cylinder surface with the interference effects of the small cylinder. For the range of Reynolds numbers normally encountered in practice namely $Re > 10^4$, the dominant component of the mean drag is due to the form drag as the result of pressure changes (Gerhart et. al., 1985). The contribution of friction drag is less than 2%-3% and thus may be omitted in the analysis. Figure 7 shows the pressure distribution along the perimeter of the main cylinder with different piggyback configurations for Reynolds number of 1.4×10^5 . The pressure distribution of the single cylinder counterpart is also plotted for comparison. The pressure coefficient in Figure 7 is defined as;

$$C_p = \frac{2(p - p_o)}{\rho U^2} \quad (4)$$

where p_o is the pressure at faraway location upstream the cylinder. It can be seen that the existence of the small cylinder has a significant effects on the mean pressure distribution on the main cylinder. The small cylinder has a minimum effect on the pressure distribution of the main cylinder when positioned directly behind the cylinder in the symmetric line ($\beta=\pi$). However, it does show a slight pressure decrease (almost negligible) on the downstream part of the cylinder. This explains the slight decrease of the mean drag coefficients for the main cylinder in Figure 3. The pressure in the front part of the cylinder reduces considerably when the small cylinder is placed in the front part of the main cylinder ($\beta=0$). This reduction in pressure continues towards the downstream part until it reaches a constant pressure in the lee-wake area. The reduction in



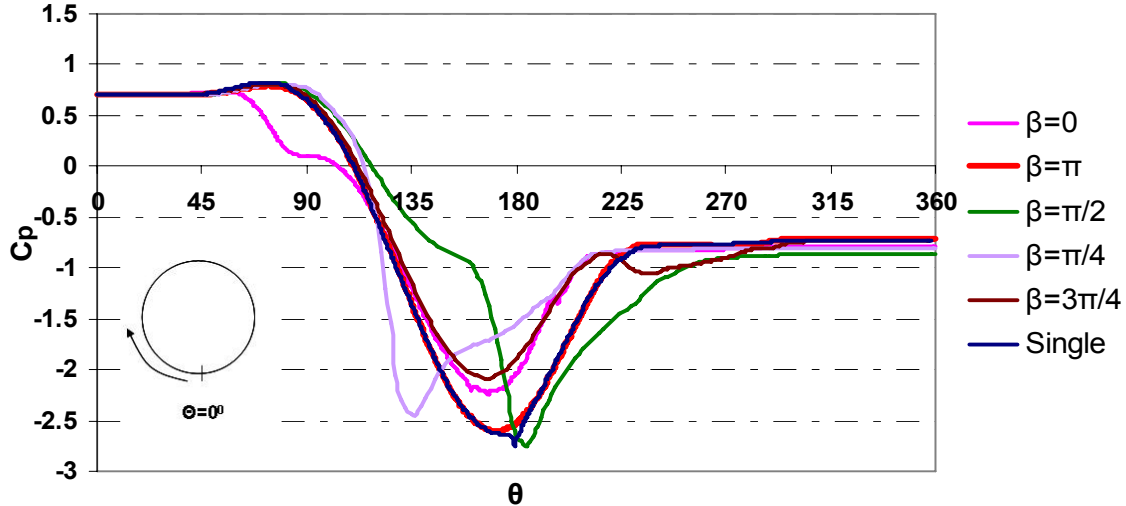


Figure 7: Pressure Distribution along Main Cylinder Surface

the wake pressure can be observed from Figure 3 when the mean drag coefficient for the main cylinder reduces with respect to the single cylinder. In the case of $\beta=\pi/2$, the decrease in the value of the pressure coefficient in the front surface ($\theta=90^\circ-160^\circ$) of the cylinder is gentle and beyond $\theta=160^\circ$ the pressure drops suddenly together with other configurations. The slow decrease in the wake pressure is due to the blockage effect of the small cylinder and the sudden drop in the pressure is the result of the acceleration effect of the flow through the gap (Tsuitsui, et al. 1997). Therefore, with this configuration the main cylinder will experience the highest drag. This non-symmetric behaviour of the pressure distribution may be the factor of the smaller mean lift as compared to the single cylinder. It is also noted that the drop in pressure for $\beta=\pi/4$ bundle contributes to the decrease in the mean drag coefficient of the main cylinder.

The separation point where the flow begins to detach from the surface can be characterized by recognizing that the separation point is associated with the lowest pressure point. This is because the flow reverses its direction in the viscous region due to the different pressure gradient and eventually detaches itself from the sheared boundary layer of the cylinder's surface. It can be noticed from the pressure distribution graph that for the single cylinder the flow separates at around 180° which is on top of the main cylinder. This is the same with $\beta=\pi$ arrangement as the small cylinder is placed beyond the separation region and thus has little effect on the location of separation point of the main cylinder. In the case of $\beta=\pi/2$, the separation point shifts slightly downstream at about 190° . The flow separates upstream with $\beta=\pi/4$ configuration at about 135° .

CONCLUSIONS

We have attempted to use computational fluid dynamics tools to study flows past pipeline bundles, and predict drag and lift forces on the pipeline. It was found that the interference of a small cylinder (e.g. umbilical) has a strong effect on the force coefficients of the main cylinder (e.g. pipeline) and on the cylinder bundle. The difference in orientation of the small cylinder highly influences the hydrodynamic characteristics of the bundle.

The main cylinder in $\beta=\pi/2$ configuration will experience the highest mean drag in comparison with other configurations and its single cylinder counterpart. The increase in drag can be up to 50% more than the single cylinder. The drag increase for the $\beta=\pi/2$ arrangement is mainly caused by the increase of the stagnation pressure and the high pressure region downstream of the cylinder. For $\beta=0$ and $\beta=\pi$, the mean drag coefficients on the main cylinder is actually smaller than the single cylinder in all cases investigated. Complementing the increase in mean drag coefficients, the main cylinder will experience a reduction in the mean lift coefficients up to 28% with $\beta=\pi/2$ arrangement. The maximum lift on the main cylinder will occur with $\beta=\pi/4$ arrangement. The mean lift will increase as the Reynolds number increases. In the case of $\beta=\pi/2$, the decrease in the value of the pressure coefficient in the front surface of the cylinder is gentle and beyond that the pressure drops suddenly. The slow decrease in the wake pressure is due to the blockage effect of the small cylinder and the sudden drop in the pressure is the results of the acceleration effect of the flow through the gap. This leads to higher drag on the main cylinder of this orientation.

The commonly used Equivalent Diameter approach was found to underestimate the total drag force on a pipeline bundle. For the $\beta=\pi/2$ arrangement, the drag on the bundle is about 18%-40% higher than its equivalent counterpart cylinder. However, the assumption corresponds fairly well with $\beta=\pi/4$ arrangement with only 10% of discrepancies. With the rest of the configurations, the total drag force obtained on the bundle is lower than the equivalent cylinder. It can also be seen that with this normalization, the small cylinder of $\beta=\pi$ and $\beta=0$ bundle recorded an almost similar drag throughout the Reynolds numbers examined. The assumption in the Equivalent Diameter concept matches quite well when the small cylinder is placed with $\beta=\pi/4$ only with some small differences in terms of the mean lift.

It is hoped that studies such as the present one will shed light on accuracy of industry wide practices for design of pipeline structures for stability and strength. In a

forthcoming paper, we propose to discuss the combined effect of waves and currents on pipeline bundles.

ACKNOWLEDGEMENTS

The study was sponsored by Woodside Energy Ltd. and JP Kenny Ltd. The support of Roland Fricke at Woodside Energy is gratefully acknowledged. The software FLUENT was made available through academic license distributed by Fluvius Ltd., Sydney.

REFERENCES

- Det Norske Veritas (DNV), 1988. "On-Bottom Stability Design of Submarine Pipelines," Recommended Practice (RP) E305, Oslo
- FLUENT User Manual, 2003.
- GERHART, P.M. and GROSS, R.J., (1985), "Fundamentals of Fluid Mechanics", Addison-Wesley Publishing Company, USA.
- KAMARUDIN, M.H. 2005. "Numerical Modelling of Hydrodynamic Coefficients for Piggyback Pipeline", *UWA Honours Thesis*, Perth.
- SAKAMOTO, H. and HANIU, H., (1994), "Optimum suppression of fluid forces acting on a circular cylinder", *Journal of Fluids Engineering*, Vol. 116, pp 221-227
- SCHLICHTING, H., (1979), "Boundary-layer theory," McGraw-Hill, 7th Edition, New York.
- SUMER, B.M. and FREDSE, J. (1997), "Hydrodynamics around Cylindrical Structures," *Advanced series on Ocean Engineering*, Vol 12, World Scientific, Singapore.
- TSUITSUI, T., IGARASHI, T. and KAMEMOTO, K., (1997), "Interactive flow around two circular cylinders of different diameters at close proximity. Experiment and numerical analysis by vortex method", *Journal of Wind Engineering and Industrial Aerodynamics*, Vol.69-71, pp 279-291.
- ZHAO, M., CHENG, L., TENG, B. and DONG, G., (2005), "Hydrodynamic forces on dual cylinders of different diameters in steady current". (Submitted to *Journal of Fluid and Structures*).